

# Effect of Different Types of Cuts on Different Parameters of Disc Brake

Anil Bakshi<sup>1</sup>, Amritpal Singh<sup>2</sup>

<sup>1</sup> M.Tech Scholar, Swami Sarvanand Institute of Engineering and Technology, Dinanagar, Punjab, India-143531

<sup>2</sup> Asst. Professor, Swami Sarvanand Institute of Engineering and Technology, Dinanagar, Punjab, India-143531

**Abstract**— The braking system is very essential in moving vehicles. In this paper, my aim is to analyze the effect of different types of cuts on different parameters of disc brake. This analysis is done using structural and fluent analysis. With the help of these analysis, we find out which cut pattern is best taking into account heat dissipation rate and strength. To achieve these objectives, ansys workbench software is used. In thermal analysis, it is found out that elliptical cuts have better heat dissipation rate. In static structural analysis, after finding out the total deformation and equivalent von misses stress, it is observe that circular cuts has better strength. In steady state thermal analysis, it is observed with the increasing of braking time the temperature increases. In wear rate analysis, wear rate is calculated by Rhee's formula. The contact pressure and wear rate is calculated by using different material in ansys workbench software.

**Keywords**— Circular cuts, disc brake, elliptical cuts, structural analysis, thermal analysis, wear rate.

## I. INTRODUCTION

Frictional brakes are used in vehicles to decelerate the vehicle; this is done by converting the kinetic energy into heat energy, which is later dissipated to surroundings. The efficiency and life of brake depends on time taken for heat dissipated, material used and forces applied on brakes. Important parameters like noise characteristics, heat flow and reliability is also taken into consideration during designing of brakes. The brakes can be designed properly by taking different composite material. Herbert Food, in 1897 designed the first brake which is constructed with the help of cotton type based material composed with bitumen solution and used for wagon wheels as well as early automobile purposes.

## II. PROBLEM FORMULATION

With the studied literature, it is observed that the heat produced during rubbing of disc pads should be dissipated regularly so that the performance of disc brake should increase. Heat dissipated depends largely on the geometrical features such as size and shape of holes on rotor. But these features should not effect the stresses produced due to holes. As we know, stress concentrations are developed in a body due to irregularities. Thus, stress concentration largely affect the mechanical behaviour of disc brakes. Therefore, it is necessary to design a braking system that should have a better heat transfer rate without compromising the mechanical strength in terms of stresses produced.

## III. OBJECTIVES

- i) With the help of Fluent analysis determine the rate of heat dissipation in different types of cuts in rotors.
- ii) With the help of Static structure analysis determine the strength of different types of cuts in rotor.
- iii) Using the Statics structural analysis finding out the contact pressure and wear rates.
- iv) Using different composition of brake pads finding out the contact pressure and wear rates.

## IV. RESEARCH METHODOLOGY

In this work for simulation and analysis we used the ansys workbench.

*Thermal Analysis:*

In Thermal Analysis, we use the fluent analysis in ansys workbench and taking the velocity of fluid entering the enclosure is 25m/s and temperature around the disc is around 550 kelvin and in thermal analysis we find the velocity and temperature counter.

*Stuctural Analysis:*

In static structural analysis, we use the ansys workbench to find the deformation, elastic strain energy, von misses stresses, sliding distance and contact pressure.

*Wear Rate Analysis:*

In wear rate analysis, we use ansys workbench. As we know the mass loss due to wear is directly related to displacement that is occurs on the rubbing surface using it will act on the normal direction. For calculating wear rate, we use Rhee's modified wear formula is

$$\Delta h = k p^a (\Omega r)^b t^c$$

where  $\Omega$  is the rotational speed and  $r$  is the mean pad mean radius. We set  $k = 1.78 \times 10^{-13} \text{ m}^3/\text{Nm}$ .

## V. RESULTS AND DISCUSSION

In fluent analysis, we consider different cuts on rotor and after that we find out which one is best suitable. We consider two types of cuts on rotor i.e. circular and elliptical cuts and then finding heat transfer rate by using ansys workbench software. Heat transfer rate increases with no. of cuts in disc because due to increase in surface area. Due to increase in no. of cuts strength of disc brake decreases. Therefore, during designing we have to keep in mind both the factors.

Fig. 1 shows the circular cut and elliptical cut patterns having the inner diameter is 120 mm and the outer diameter is 240 mm respectively. We make this geometry and then

imported these models into ansys fluent models for thermal analysis.

1. Geometry
2. Meshing
3. CFD problem and solution

Geometry fluid enclosure is created around the disc geometry fluid enclosure is created with length equal to two times from the rear edge of the disc. This helps into simulate the flow around disc.

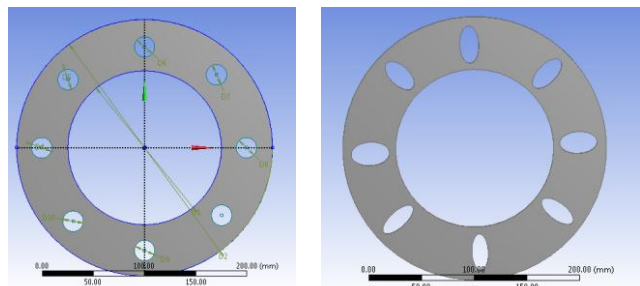


Fig. 1. Two models with circular and elliptical cut patterns.

Mesh size influences various parameters of the solution. That's why, we select fine mesh for accurate results. If the mesh size is not accurate then solution will not be proper. Fig. 2 shows the fine mesh of circular and elliptical cuts in ansys workbench software using fluent analysis.

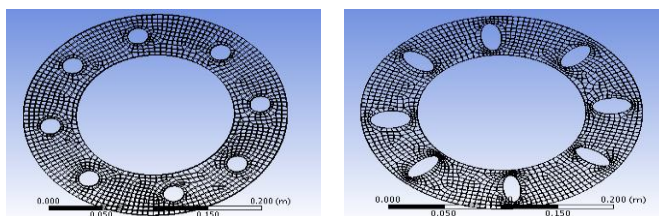


Fig. 2. Fine mesh for circular and elliptical cut pattern.

**CFD Problem setup and solution:** In this problem, we considered that the fluid enters with the velocity of 35 m/s and around the disc temperature is 550 k. This problem is solved by 450 iteration pressure based solution method and after it K-epsilon model is applied then followed by turbulence flow. In the Fig. 3 shows temperature variation of circular and elliptical crossection. In figures it is clearly shown that circular cut pattern has dense dots near cuts due to this air that enters into the cuts does not leave easily. But in case of elliptical cuts there are less dots because air circulation through the cuts is better.

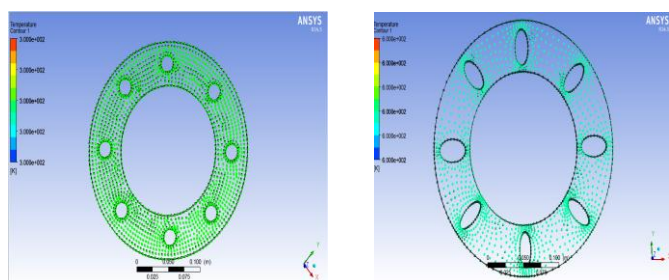


Fig. 3. Temperature contour for the circular and elliptical cut patterns.

Fig. 4 shows velocity contour for elliptical and circular disc. From this it is clearly seen that the layer of circular disc is large and layer of elliptical cuts disc is small. This observation tells us that more heat is dissipated in elliptical cuts because it allows more fresh air to come in contact with disc and more heat is dissipated as comparison with circular cuts.

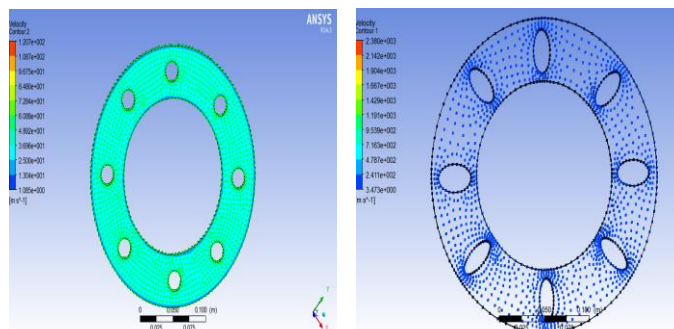


Fig. 4. Velocity contour for circular and elliptical cut patterns.

**Analyze the effect of strength on different types of cuts in rotor by using the static structural analysis:** Now after doing thermal analysis it is very important to do structural analysis of discs having circular and elliptical cuts. This analysis is important because it is necessary to check whether the disc can withstand braking force and how the disc behaves under these situations.

First step is to import the model having same material into the static structural of ansys workbench software. We have to take the fine mesh analysis for the better result. In this analysis, we considered that the inner surface of the disc is fixed and then the load is applied on it and after that we do analysis for the total deformation and equivalent von mises stresses, directional deformation and elastic strains which is shown in figures. It is clearly visible in Fig. 5 that the deformation is more at the outer edge and lower at the inner edge. It shows that maximum value of deformation in case for circular type cut is  $1.0111 \times 10^{-10}$  m whereas in case of elliptical type cut is  $1.3336 \times 10^{-10}$  m which shows that there is more deformation in case of elliptical cuts as compared to circular.

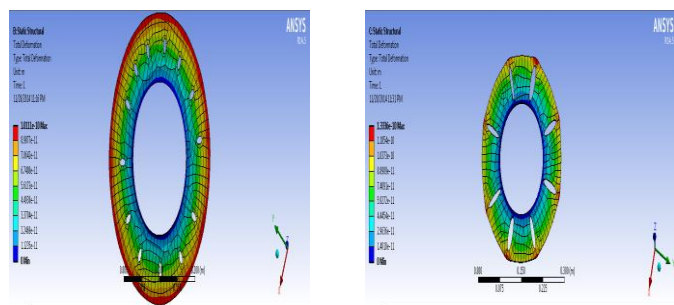


Fig. 5. Deformation in circular and elliptical cut sections.

In the Fig. 6 the stresses value of circular and elliptical cuts is given. The stress value in case of circular cut is 1254.5 Pa while in elliptical cut it is 1327.1 Pa. The results shows that there will be more stresses produced in elliptical cuts which means elliptical cuts are weaker as compared to circular cuts

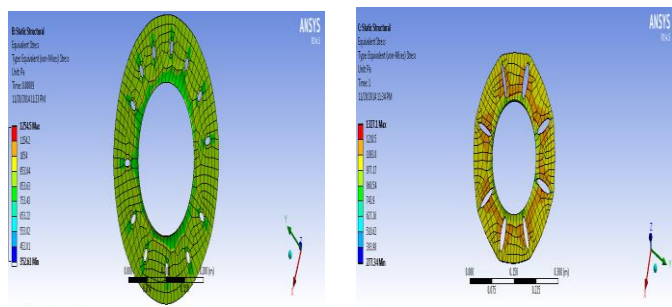


Fig. 6. Von misses stresses in circular cut and elliptical cut sections.

Fig. 7 shows that the equivalent strain energy in case of both circular and elliptical types of cut pattern. In case of circular types of cut pattern, the maximum strain energy found to be  $7.2673 \times 10^{-9}$  Joule and in case of elliptical  $7.7889 \times 10^{-9}$  joule which shows that there will be more deformation in elliptical cut patterns

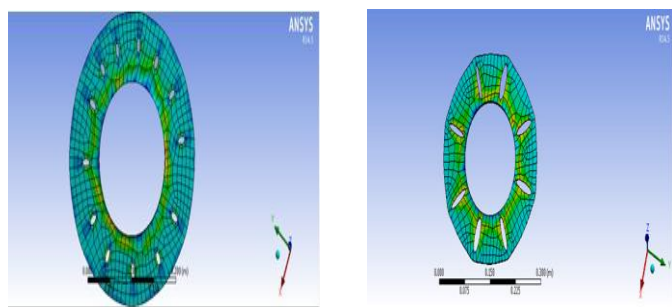


Fig. 7. Elastic strain energy for circular cut and elliptical cut pattern.

**Wear rate analysis:** Now after doing thermal and structural analysis, we have to do wear rate analysis so that we can find out which type of cut is best suitable. In this analysis, we considered the disc of plain carbon steel and the brake shoe of different composition and finding out which one is best. First we make the design of rotor and after that giving it the rotational velocity and then attach brake shoes at the both sides of rotor. Then we will vary the composition of brake material. This results in evaluating the deformation and von misses stresses and finally calculating wear rate. The loss of mass due to wear is directly related to displacement which is occurring on the rubbing surface that is acting on the normal direction. Using the Rhee's modified wear formula which is

$$\Delta h = k p^a (\Omega r)^b t^c$$

In this case  $\Omega$  is the rotational speed and  $r$  is the mean pad mean radius. In this simulation the wear rate coefficient is set to be  $k = 1.58 \times 10^{-13} \text{ m}^3/\text{Nm}$ . From this analysis, we have to calculate the contact pressure using ansys. In this we consider the three rotors having circular cut, elliptical cuts pattern and the simple rotor without any cuts. These are shown in figures.

Import these geometry one by one into the static structural analysis in ansys workbench and after importing into the static structural mesh the whole model for the structural analysis. Now below in Fig. 9 shows fine mesh for three different models mesh. Now the next step is to give rotational speed and applying pressure on the brake pads and then calculating von misses stress, sliding distance directional deformation and contact pressure. The parameter which we have to input is coefficient of friction and analysis is done on this basis.

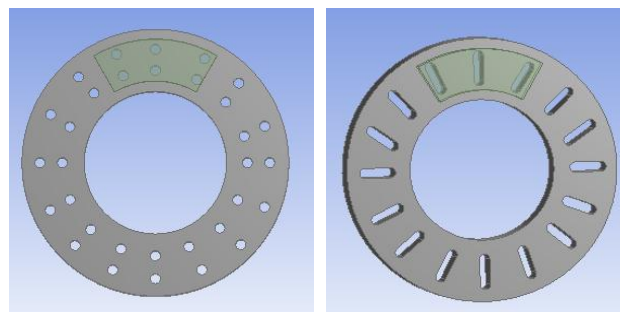
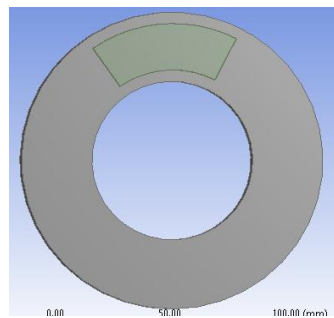


Fig. 8. The simple rotor without any cuts, with circular cuts and elliptical cuts.

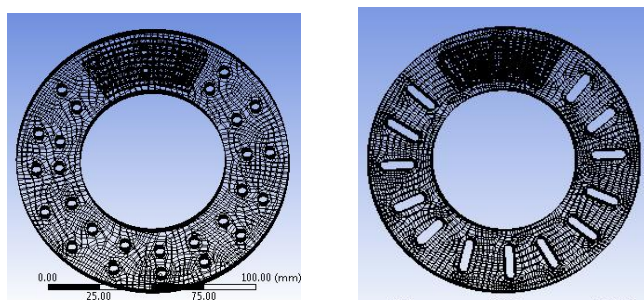
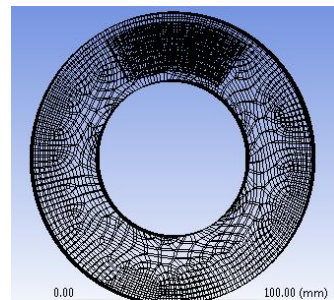


Fig. 9. Fine mesh for disc rotor without any cut, with circular cuts and with elliptical cut patterns.

After the meshing of three rotors, we have to fix brake shoe and after giving rotational velocity we have to apply pressure on both sides of brake pads. Then this results in finding the contact pressure. Fig. 10, 11 shows that the equivalent stresses, directional deformation, sliding distance and contact pressure using the ansys software

It shows the stresses produced in a simple rotor that does not have any cuts. It is clear from figure that there is maximum stress at lower edge and minimum at outer edge. Moreover, the stresses are uniform due to uniform cross-section because there are no cuts that increases more stresses. Fig 11 shows the directional deformation in a simple rotor that doesn't have any cuts. It shows that on one side of simple

rotor have maximum deformation and on another side have minimum deformation.

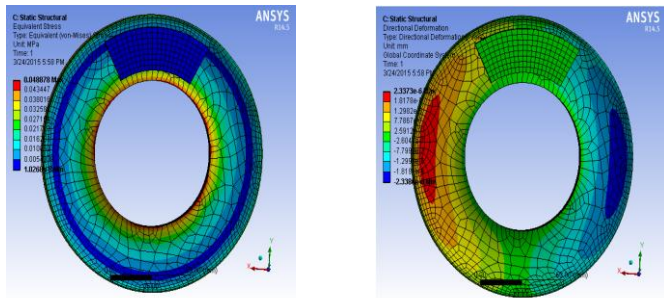


Fig. 10. Shows the equivalent stress and the directional deformation of simple rotor.

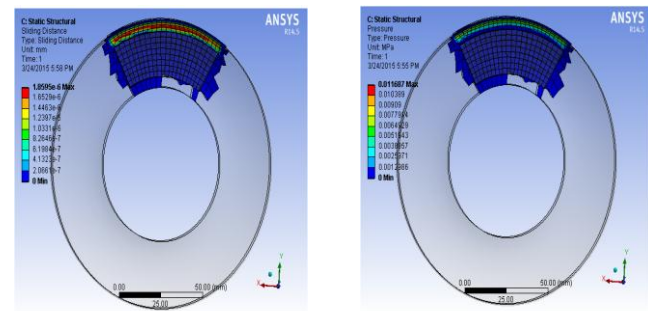


Fig. 11. Shows the sliding distance and contact pressure of simple rotor.

Fig. 11 shows the sliding distance that going to take place in the simple rotor. Sliding distance is the total distance covered by a disc during braking time. Fig. 12 shows the contact pressure in the simple rotor. It arises when there is surface contact between the two bodies. Contact pressure is more near area where brake pad applied the force on rotor.

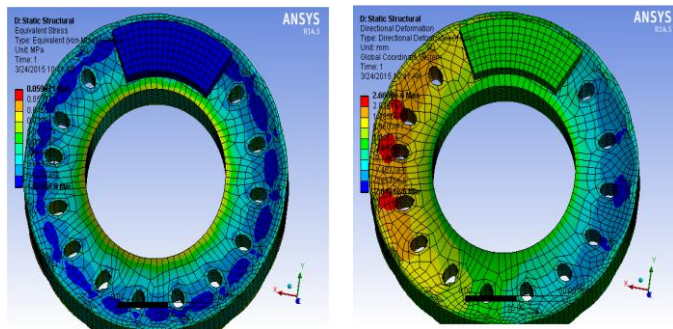


Fig. 12. Equivalent stresses and directional deformation for circular cut patterns.

Fig. 12 shows the stresses produced in a rotor having circular cuts. It clearly shows there is maximum stress at lower edge and minimum at outer edge. Moreover, there is increase in stresses in middle portion due to circular cuts. Fig. 12 shows the directional deformation in rotor having circular cuts. It shows that on one side of rotor the deformation is maximum and on another side deformation is minimum. Moreover, it is clear from above figures that that area of max. and min. deformation decreases due to circular cuts.

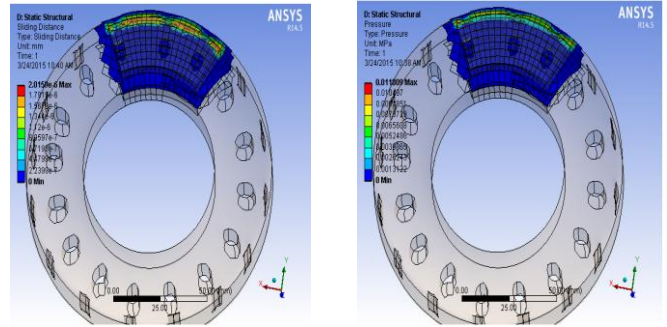


Fig. 13. Sliding distances and contact pressure for circular cuts pattern.

Fig. 13 shows the sliding distance and contact pressure in the rotor having circular cuts.

Now consider a brake rotor having elliptical cuts and after applying contact pressure on both sides, we have to give rotational velocity to the rotor.

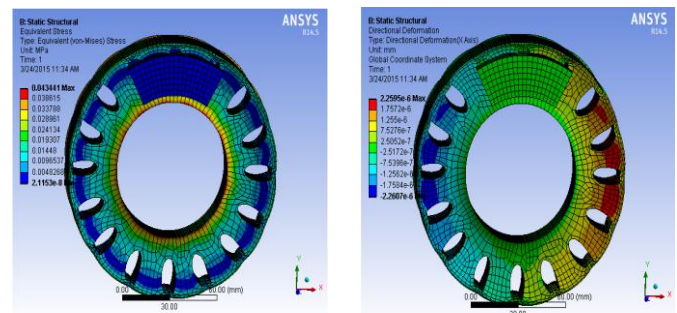


Fig. 14. Equivalent stresses and directional deformation for elliptical cuts rotor.

Fig. 14 shows the stress produced in rotor having elliptical cuts. It shows that there is maximum stress at lower edge and minimum at outer edge. Due to elliptical cuts stresses increased as compared to circular cuts. Fig. 14 shows the directional deformation in rotor having elliptical cuts. It shows that on one side of rotor the deformation is maximum and on another side deformation is minimum. Moreover, it is clear from fig. that that area of max. and min. deformation decreases due to elliptical cuts

Fig. 15 shows the sliding distance that is taken place due to elliptical cuts. Fig. 15 shows the contact pressure in case of elliptical cuts.

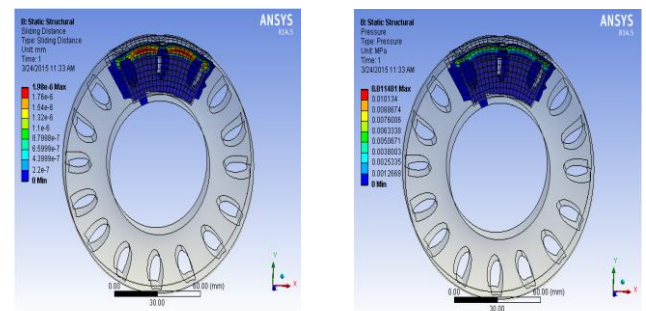


Fig. 15. Sliding distance and directional deformation for elliptical cuts pattern.

*Finding the contact pressure and wear rates by using the different composition of brakes pads:*

TABLE I. Show mechanical properties of different composition of material for brakes pad.

Materials	Young modulus (GPa)	Poisson ratio	Elastic limit (Mpa)	Yield strength (Mpa)	Ultimate tensile strength (Mpa)	Strain	Braking strain
Ferritic steel	206	0.28	450	500	550	0.04	0.106
Pearlitic steel	206	0.28	520	800	920	0.04	0.106
Iron oxide	380	0.3	290	305	340	0.008	0.009
Graphite	20	0.3	15	35	45	0.05	0.15
Soft copper	120	0.35	175	185	215	0.03	0.11
Sic	150	0.35	3000	4325	5000	0.06	0.18

TABLE II. Shows the wear rate of brake pads made of ferritic materials and disc made of plain carbon steel taking  $\mu$  value 0.3 (Having No Cuts).

$\mu$	Rpm	Pressure	Directional deformation (mm)	Equivalent von misses stress (Mpa)	Contact pressure (Mpa)	Sliding distance (mm)	Wear ( $M^3/m$ )
0.30	800	3MPa	$2.7473 \times 10^{-6}$	0.038878	0.011724	$1.8605 \times 10^{-6}$	$9.6798 \times 10^{-13}$
0.30	1000	3MPa	$3.9521 \times 10^{-6}$	0.066371	0.018651	$2.9155 \times 10^{-6}$	$1.4286 \times 10^{-12}$
0.30	1200	3MPa	$5.7591 \times 10^{-6}$	0.09997	0.026305	$4.2039 \times 10^{-6}$	$3.0072 \times 10^{-12}$

TABLE III. Shows the wear rate of brake pads made of ferritic materials and disc of plain carbon steel taking  $\mu$  value 0.35 (Having No Cuts).

$\mu$	Rpm	Pressure	Directional deformation (mm)	Equivalent von misses stress (Mpa)	Contact pressure (Mpa)	Sliding distance (mm)	Wear ( $M^3/m$ )
0.35	800	3MP	$2.2412 \times 10^{-6}$	0.043862	0.011767	$1.8542 \times 10^{-6}$	$9.8045 \times 10^{-13}$
0.35	1000	3MP	$3.1214 \times 10^{-6}$	0.074631	0.018987	$2.8824 \times 10^{-6}$	$1.8346 \times 10^{-12}$
0.35	1200	3MP	$5.1400 \times 10^{-6}$	0.11497	0.024324	$4.1651 \times 10^{-6}$	$3.0547 \times 10^{-12}$

TABLE IV. Shows the wear rate of brake padmade of ferritic materials and disc of plain carbon steel taking  $\mu$  value 0.40(Having No Cuts).

$\mu$	Rpm	Pressure	Directional deformation (mm)	Equivalent von misses stress (Mpa)	Contact pressure (Mpa)	Sliding distance (mm)	Wear ( $M^3/m$ )
0.40	800	3MP	$2.3674 \times 10^{-6}$	0.049276	0.012021	$1.8567 \times 10^{-6}$	$9.8143 \times 10^{-13}$
0.40	1000	3MP	$3.6875 \times 10^{-6}$	0.078568	0.019013	$2.8827 \times 10^{-6}$	$1.8453 \times 10^{-12}$
0.40	1200	3MP	$5.4567 \times 10^{-6}$	0.12397	0.028071	$4.1748 \times 10^{-6}$	$3.0705 \times 10^{-12}$

TABLE V. Shows the wear rate of brake pads made of ferritic materials and disc of plain carbon steel taking  $\mu$  value 0.30(Circular Cuts).

$\mu$	Rpm	Pressure	Directional deformation (mm)	Equivalent von misses stress (Mpa)	Contact pressure (Mpa)	Sliding distance (mm)	Wear ( $M^3/m$ )
0.30	800	3MP	$2.6760 \times 10^{-6}$	0.059543	0.011802	$2.0445 \times 10^{-6}$	$9.4767 \times 10^{-13}$
0.30	1000	3MP	$4.1860 \times 10^{-6}$	0.093494	0.018762	$3.19234 \times 10^{-6}$	$1.1067 \times 10^{-12}$
0.30	1200	3MP	$6 \times 10^{-6}$	0.13566	0.026456	$4.5655 \times 10^{-6}$	$2.9823 \times 10^{-12}$

TABLE VI. It shows the wear rate of brake pads made of ferritic materials and disc of plain carbon steel taking  $\mu$  value 0.35 (Circular Cuts).

$\mu$	Rpm	Pressure	Directional deformation (mm)	Equivalent von misses stress (Mpa)	Contact pressure (Mpa)	Sliding distance (mm)	Wear ( $M^3/m$ )
0.35	800	3MP	$2.6660 \times 10^{-6}$	0.059821	0.011809	$2.0159 \times 10^{-6}$	$9.6927 \times 10^{-13}$
0.35	1000	3MP	$4.1660 \times 10^{-6}$	0.093471	0.018452	$3.1499 \times 10^{-6}$	$1.6464 \times 10^{-12}$
0.35	1200	3MP	$5.9998 \times 10^{-6}$	0.1346	0.026571	$4.5359 \times 10^{-6}$	$3.0053 \times 10^{-12}$

TABLE VII. Shows the wear rate of brake pads made of ferritic materials and disc of plain carbon steel taking  $\mu$  value 0.40 (Circular Cuts).

$\mu$	Rpm	Pressure	Directional deformation (mm)	Equivalent von misses stress (Mpa)	Contact pressure (Mpa)	Sliding distance (mm)	Wear ( $M^3/m$ )
0.40	800	3MP	$2.6450 \times 10^{-6}$	0.06421	0.011929	$2.0273 \times 10^{-6}$	$9.7517 \times 10^{-13}$
0.40	1000	3MP	$4.1679 \times 10^{-6}$	0.09677	0.018752	$3.1346 \times 10^{-6}$	$1.7658 \times 10^{-12}$
0.40	1200	3MP	$5.9818 \times 10^{-6}$	0.13567	0.024771	$4.5656 \times 10^{-6}$	$3.0453 \times 10^{-12}$

TABLE VIII. Shows the wear rate of brake pads made of ferritic materials and disc of plain carbon steel taking  $\mu$  value 0.30 (elliptical cuts).

$\mu$	Rpm	Pressure	Directional deformation (mm)	Equivalent von misses stress (Mpa)	Contact pressure (Mpa)	Sliding distance (mm)	Wear ( $M^3/m$ )
0.30	800	3MP	$2.2685 \times 10^{-6}$	0.045741	0.01231	$1.9765 \times 10^{-6}$	$9.2330 \times 10^{-13}$
0.30	1000	3MP	$3.5674 \times 10^{-6}$	0.067857	0.017814	$3.0677 \times 10^{-6}$	$1.0181 \times 10^{-12}$
0.30	1200	3MP	$5.0928 \times 10^{-6}$	0.098243	0.026598	$4.4654 \times 10^{-6}$	$2.7382 \times 10^{-12}$

TABLE IX. Shows that wear rate of brake pads made of ferritic materials and disc of plain carbon steel taking  $\mu$  value 0.35 (elliptical cuts).

$\mu$	Rpm	Pressure	Directional deformation (mm)	Equivalent von misses stress (Mpa)	Contact pressure (Mpa)	Sliding distance (mm)	Wear ( $M^3/m$ )
0.35	800	3MP	$2.2824 \times 10^{-6}$	0.043461	0.011241	$1.9718 \times 10^{-6}$	$9.377 \times 10^{-13}$
0.35	1000	3MP	$3.5464 \times 10^{-6}$	0.067856	0.018214	$3.0743 \times 10^{-6}$	$1.0912 \times 10^{-12}$
0.35	1200	3MP	$5.0927 \times 10^{-6}$	0.097781	0.025698	$4.4564 \times 10^{-6}$	$2.8382 \times 10^{-12}$

TABLE X. Shows the wear rate of brake pads made of ferritic materials and disc of plain carbon steel taking  $\mu$  value 0.40 (elliptical cuts).

$\mu$	Rpm	Pressure	Directional deformation (mm)	Equivalent von misses stress (Mpa)	Contact pressure (Mpa)	Sliding distance (mm)	Wear (M <sup>3</sup> /m)
0.40	800	3MP	$2.2687 \times 10^{-6}$	0.043621	0.011741	$1.9832 \times 10^{-6}$	$9.482 \times 10^{-13}$
0.40	1000	3MP	$3.5468 \times 10^{-6}$	0.067927	0.01924	$3.1227 \times 10^{-6}$	$1.1802 \times 10^{-12}$
0.40	1200	3MP	$5.0878 \times 10^{-6}$	0.0977853	0.027598	$4.4859 \times 10^{-6}$	$2.9992 \times 10^{-12}$

TABLE XI. Shows the wear rate of brake pads made of pearlitic materials and disc of plain carbon steel taking  $\mu$  value 0.35.

$\mu$	Rpm	Pressure	Directional deformation (mm)	Equivalent von misses stress (Mpa)	Contact pressure (Mpa)	Sliding distance (mm)	Wear (M <sup>3</sup> /m)
0.35	800	3MP	$2.2764 \times 10^{-6}$	0.043441	0.011401	$1.9708 \times 10^{-6}$	$9.57 \times 10^{-13}$
0.35	1000	3MP	$3.5454 \times 10^{-6}$	0.067876	0.017814	$3.0794 \times 10^{-6}$	$1.7882 \times 10^{-12}$
0.35	1200	3MP	$5.0927 \times 10^{-6}$	0.09821	0.02498	$4.424 \times 10^{-6}$	$3.0952 \times 10^{-12}$

TABLE XII. Shows the wear rate of brake pads made of graphite materials and disc of plain carbon steel taking  $\mu$  value 0.35.

$\mu$	Rpm	Pressure	Directional deformation (mm)	Equivalent von misses stress (Mpa)	Contact pressure (Mpa)	Sliding distance (mm)	Wear (M <sup>3</sup> /m)
0.35	800	3MP	$2.6544 \times 10^{-6}$	0.060828	0.0056098	0.005810	$4.1651 \times 10^{-13}$
0.35	1000	3MP	$4.1675 \times 10^{-6}$	0.093682	0.0073465	$2.9832 \times 10^{-6}$	$1.0651 \times 10^{-12}$
0.35	1200	3MP	$5.9998 \times 10^{-6}$	0.13561	0.013447	$4.3573 \times 10^{-6}$	$2.7271 \times 10^{-12}$

TABLE XIII. Shows the wear rate of brake pads made of iron oxide materials and disc of plain carbon steel taking  $\mu$  value 0.3.

$\mu$	Rpm	Pressure	Directional deformation (mm)	Equivalent von misses stress (Mpa)	Contact pressure (Mpa)	Sliding distance (mm)	Wear (M <sup>3</sup> /m)
0.35	800	3MP	$2.6660 \times 10^{-6}$	0.059821	0.01281	$2.0162 \times 10^{-6}$	$9.8873 \times 10^{-13}$
0.35	1000	3MP	$4.1660 \times 10^{-6}$	0.092471	0.019453	$3.152 \times 10^{-6}$	$1.8679 \times 10^{-12}$
0.35	1200	3MP	$5.9998 \times 10^{-6}$	0.13246	0.027572	$4.538 \times 10^{-6}$	$3.0824 \times 10^{-12}$

TABLE XIV. It shows that wear rate of brake pads made of soft copper materials and disc of plain carbon steel taking  $\mu$  value 0.35.

$\mu$	Rpm	Pressure	Directional deformation (mm)	Equivalent von misses stress (Mpa)	Contact pressure (Mpa)	Sliding distance (mm)	Wear (M <sup>3</sup> /m)
0.35	800	3MP	$2.6624 \times 10^{-6}$	0.059019	0.015187	$1.9391 \times 10^{-6}$	$1.2192 \times 10^{-13}$
0.35	1000	3MP	$4.1623 \times 10^{-6}$	0.096068	0.024061	$3.0244 \times 10^{-6}$	$1.8579 \times 10^{-12}$
0.35	1200	3MP	$5.9894 \times 10^{-6}$	0.13509	0.033769	$4.3451 \times 10^{-6}$	$3.7893 \times 10^{-12}$

TABLE XV. Shows the wear rate of brake pads of Sic materials and disc of plain carbon steel taking  $\mu$  value 0.35.

$\mu$	Rpm	Pressure	Directional deformation (mm)	Equivalent von misses stress (Mpa)	Contact pressure (Mpa)	Sliding distance (mm)	Wear (M <sup>3</sup> /m)
0.35	800	3MP	$2.6684 \times 10^{-6}$	0.06119	0.015114	$1.9399 \times 10^{-6}$	$1.2312 \times 10^{-13}$
0.35	1000	3MP	$4.1703 \times 10^{-6}$	0.093968	0.023503	$3.0323 \times 10^{-6}$	$1.2683 \times 10^{-12}$
0.35	1200	3MP	$5.9994 \times 10^{-6}$	0.13489	0.034057	$4.3676 \times 10^{-6}$	$2.5893 \times 10^{-12}$

The above tables shows the wear rates of disc having no cuts, circular cuts and elliptical cuts under various circumstances. From these readings, it is observed that wear rate in case of elliptical cut is less. The reason behind it is thermal dissipation, as it is observed in thermal analysis that elliptical cut pattern has more heat dissipation. Due to more heat dissipation, wear rate is less because brake pad has to work on less temperature and due to this life of brake pad increases.

In above following tables, we have taken different coefficient of friction for different materials. As we know, coefficient of friction plays an important role in selection of braking material. From above tables, it is observed that for different braking material, SiC material brake pad has less wear rate when we use disc made of plain carbon steel.

## VI. CONCLUSION

It is concluded from the studies so far that various cuts of various geometry has better heat transfer rate and strength. In thermal analysis, it is concluded that there is better heat dissipation in case of disc rotor made of plain carbon steel having elliptical cuts as compared to circular cuts. The main reason behind this conclusion is elliptical cuts have more

surface area as compared to circular cuts. This is based on Newton's Law of Cooling. Due to this more air will strike the discs and and this results in better heat dissipation.

In structural analysis, elliptical cuts are weaker as compared to circular cut patterns. The stresses produced in elliptical cuts are more because these elliptical cuts cannot withstand higher force after prolonged application. The stress concentration is less in case of circular cuts pattern because of regular shape in case of elliptical cuts. Therefore, it is ideal to say circular cuts are stronger.

In wear analysis, parameters like contact pressure, coefficient of friction plays an important role. As coefficient of friction increases, wear rate increases. Wear rate is less in case of elliptical cut pattern. The reason behind it is thermal dissipation, as it is observed in thermal analysis that elliptical cut pattern has more heat dissipation. Due to more heat dissipation, wear rate is less because brake pad has to work on less temperature and due to this life of brake pad increases. For selecting best material, we have taken different coefficient of friction for different materials. As we know, coefficient of friction plays an important role in selection of braking material. From above tables, it is observed that for different braking material, SiC material brake pad has less wear rate

when we use disc made of plain carbon steel. Therefore from studies it is concluded that for better heat transfer rate, better structural strength and for better wear rate we have to optimize the brakes according to the observed results.

#### ACKNOWLEDGMENT

I would like to place on record my deep sense of gratitude to Mr. Amritpal Singh, Deptt. of Mechanical Engineering, Swami Sarvanand Institute of Engineering and Technology, Dinanagar, Punjab, India for his generous guidance, help and useful suggestions. I express my sincere gratitude to Mohit Mahajan, for his stimulating guidance, continuous encouragement and supervision throughout the course of present work.

#### REFERENCES

- [1] G. Babukanth, "Transient analysis of disk brake by using ansys software," *International Journal of Mechanical and Industrial Engineering (IJMIE)*, ISSN No. 2231-6477, vol. 2, issue 1, 2012.
- [2] A. I. Dmitriev, "About the influence of automotive brake pad composition on frictional performance on nano scale modeling" *Nanosystems: Physics, Chemistry, Mathematics*, vol. 2, pp. 58-64, 2011.
- [3] Libo Tang, "Simulation analysis of train disc brake temperature field," *The 2<sup>nd</sup> International Conference on Computer Application and System Modeling*, 2012.
- [4] M. Sudhir, "Modeling an analysis for wear performance in dry sliding of Epoxy/glass/PTW composites using full factorial techniques," *Wear*, vol. 575, pp. 1-20, 2002.
- [5] Bhabani K. Satapathy, "Analysis of simultaneous influence of operating variables on abrasive wear of phenolic composites" *Wear*, vol. 253, pp. 787-794, 2002.
- [6] Bhabani K. Satapathy, "Wear data analysis of friction materials to investigate the simultaneous influence of operating parameters and compositions," *Wear*, vol. 256, pp.797-804, 2004.
- [7] Adam Adamowicz, "Influence of convective cooling on a disc brake temperature distribution during Repetitive braking," *Applied Thermal Engineering*, vol. 31, pp. 2177-2185, 2011.
- [8] P. Liu, H. Zheng, "Analysis of disc brake squeal using the complex Eigen value method," *Applied Acoustics*, vol. 68, pp. 603-615, 2007.
- [9] Choe-Yung, "Analysis of friction excited vibration of drum brake squeal," *International Journal of Mechanical Sciences*, vol. 67, pp. 59-69, 2013.
- [10] Yun Cheol Kim, "The effect of phenol resin, potassium titanate, and CNSL on the tribological properties of brake friction materials," *Wear*, vol. 264, pp. 204-210, 2008.
- [11] Gewen Yi, "Mechanical and tribological properties of phenolic resin-based friction composites filled with several inorganic fillers," *Wear*, vol. 262, pp. 121-129, 2007.
- [12] Yafei Lu, "A combinatorial approach for automotive friction materials: Effects of ingredients on friction performance" *Composites Science and Technology*, vol. 66, pp. 591-598, 2006.
- [13] Ali Belhocine, "Thermal analysis of a solid brake disc," *Applied Thermal Engineering*, vol. 32, pp. 59-67, 2012.
- [14] Aleksander Yevtushenko, "Influence of thermal sensitivity of the materials on temperature and thermal stresses of the brake disc with thermal barrier coating," *International Communications in Heat and Mass Transfer*, vol. 87, pp. 288-294, 2017.
- [15] M. Boniardi, "Failure analysis of a motorcycle brake disc," *Engineering Failure Analysis*, vol. 13, pp. 933-945, 2006.
- [16] G. Cueva, "Wear resistance of cast irons used in brake disc rotors," *Wear*, vol. 255, pp. 1256-1260, 2003.
- [17] Vlastimil Matejka, "Effects of silicon carbide particle sizes on friction-wear properties of friction composites designed for car brake lining applications," *Tribology International*, vol. 43, pp. 144-151, 2010.
- [18] Miha Pevecml, "Elevated temperature low cycle fatigue of grey cast iron used for automotive brake discs," *Engineering Failure Analysis*, vol. 42, pp. 221-230, 2014.
- [19] Anders Söderberg, "Simulation of wear and contact pressure distribution at the pad-to-rotor interface in a disc brake using general purpose finite element analysis software," *Wear*, vol. 267, pp. 2243-2251, 2009.
- [20] W. O. Sterle, "Towards a better understanding of brake friction materials," *Wear*, vol. 263, pp. 1189-1201, 2007.
- [21] Jens Wahlström, "A comparison of measured and simulated friction, wear, and particle emission of disc brakes," *Tribology International*, vol. 92, pp. 503-511, 2015.
- [22] H. B. Yan, "Role of cross-drilled holes in enhanced cooling of ventilated brake discs," *Applied Thermal Engineering*, vol. 91, pp. 318-333, 2015.
- [23] Aleksander Yevtushenko, "Temperature and thermal stresses in a pad/disc during braking," *Applied Thermal Engineering*, vol. 30, pp. 354-359, 2010.
- [24] A. A. Yevtushenko, "3D FE model of frictional heating and wear with a mutual influence of the sliding velocity and temperature in a disc brake," *International Communications in Heat and Mass Transfer*, vol. 62, pp. 37-44, 2015.
- [25] A. A. Yevtushenko, "Mutual influence of the sliding velocity and temperature in frictional heating of the thermally nonlinear disc brake," *International Journal of Thermal Sciences*, vol. 102, pp. 254-262, 2016.
- [26] A. A. Yevtushenko, "Temperature in the railway disc brake at a repetitive short-term mode of Braking," *International Communications in Heat and Mass Transfer*, vol. 84, pp. 102-109, 2017.
- [27] Piyush Chandra Verma, "Braking pad-disc system: Wear mechanisms and formation of wear fragments," *Wear*, vol. 322-323, pp. 251-258, 2015.
- [28] J. R. Laguna-Camacho, "A study of the wear mechanisms of disk and shoe brake pads," *Engineering Failure Analysis*, vol. 56, pp. 348-359, 2015.
- [29] Zmago Stadler, "Friction and wear of sintered metallic brake linings on a C/C-SiC composite brake disc," *Wear*, vol. 265, pp. 278-285, 2008.
- [30] Maurice I. Ripley, "Residual stresses in a cast iron automotive brake disc rotor," *Physica B*, vol. 385-386, pp. 604-606, 2006.
- [31] Zhen-cai Zhu, "Three-dimensional transient temperature field of brake shoe during hoist's Emergency braking," *Applied Thermal Engineering*, vol. 29, pp. 932-937, 2009.